NASA TECHNICAL MEMORANDUM

NASA TM X- 73984

NASA TM X- 73984

VORTEX SIMULATION OF THE PRESSURE FIELD OF A JET

by

Y. T. Fung* and C. H. Liu

(NASA-TM-X-73984) VORTEX SIMULATION OF THE PRESSURE FIELD OF A JET (NASA) 29 p HC A03/MF A01 CSCL 01A

N77-11989

Unclas

G3/02 54510

*NAS-NRC/NASA Research Associate

National Aeronautics and Space Administration

Langley Research Center
Hampton, Virginia 23665

1. Report No. TMX 73984	2. Government Accession No.	3. Recipient's Catalog No.
4. Title and Subtitle: Vortex Simulation of the Pressure Field of a Jet		5. Report Date: November 1976
		6. Performing Organization Code: 2620
7. Author(s): Y. T. Fung and C. H. Liu		8. Performing Organization Report No.
		10. Work Unit No.: 505-03-11-02
9. Performing Organization Name and Address: NASA-Langley Research Center, Hampton, Virginia 23665		11. Contract or Grant No.: N/A
		13. Type of Report and Period Covered: Tech. Memo.
12. Sponsoring Agency Name and Address: National Aeronautics and Space Administration, Washington, D. C. 20546		14. Sponsoring Agency Code

15. Supplementary Notes

To be presented at the 92nd ASA Meeting to be held in San Diego, CA in November 1976.

16. Abstract

Fluctuations of the pressure field of a jet are simulated numerically by a flow model consisting of axisymmetric vortex rings with viscous cores submerged in an inviscid uniform stream. Vortex shedding time intervals, randomly created to imitate the time-history characteristics of the pressure signals of a jet, are generated based on a probability distribution of the intervals between successive pressure peaks obtained from experiments. It is found that, up to five diameters downstream of the jet exit, the characteristics of the pressure fluctuations and the most probable time intervals between experimental and numerical results show good qualitative agreements. The role played by the axisymmetric vortex model in pressure field as well as extensions of the model is also discussed.

17. Key Words (Suggested by Author(s)): vortex ring, subsonic jet, pressure signal, numerical simulation	18. Distribution Statement: Unclassified Unlimited

19. Security Classif. (of this report)	20. Security Classif. (of this page)	21. No. of Pages	22. Price*
Unclassified	Unclassified	26	$3.75

* For sale by the National Technical Information Service, Springfield, Virginia 22161

VORTEX SIMULATION OF THE PRESSURE FIELD OF A JET

Y. T. Fung* and C. H. Liu
NASA Langley Research Center
Hampton, Virginia

ABSTRACT

Fluctuations of the pressure field of a jet are simulated numerically by a flow model consisting of axisymmetric vortex rings with viscous cores submerged in an inviscid uniform stream. Vortex shedding time intervals, randomly created to imitate the time-history characteristics of the pressure signals of a jet, are generated based on a probability distribution of the intervals between successive pressure peaks obtained from experiments. It is found that, up to five diameters downstream of the jet exit, the characteristics of the pressure fluctuations and the most probable time intervals between experimental and numerical results show good qualitative agreements. The role played by the axisymmetric vortex model in pressure field as well as extensions of the model is also discussed.

* NAS-NRC/NASA Research Associate

Symbols

D	Diameter of the jet nozzle
E	Complete elliptical integral of the second kind
J_o	Bessel function of the first kind of order zero
J_1	Bessel function of the first kind of order one
K	Complete elliptical integral of the first kind
P	Point of interest
p	Fluctuating pressure
p_∞	Unperturbed pressure
R	Radial position of vortex rings
r	Radial coordinate
r_1	The shortest distance from P to the center of vortical cores
r_2	The longest distance from P to the center of vortical cores
t_k	Shedding time of the k-th vortex ring
U_c	Convection velocity of vortex rings
U_∞	Velocity of the uniform stream
W_1	Induced velocity in radial direction
W_3	Induced velocity in axial direction
Z	Axial position of vortex rings
Z_{max}	Downstream distance for destruction of vortex rings
z	Axial coordinate
α	Decaying rate of the circulation of vortex rings
Γ	Circulation of vortex rings
δ	Effective radius of vortical cores
ν	viscosity

ρ	Density of the fluid
τ	Time scale
ϕ	Velocity potential
ψ	Stream function

INTRODUCTION

The concept of modeling turbulent jets in terms of some well-defined patterns has been proposed by many researchers as a way to attack the problem of jet noise generation and its suppression. Based on the experimental observations that pressure fluctuations outside the mixing region come in rather well-organized packages, Mollo-Christensen[1] first suggested that certain natural organized structures might exist within the shear flow turbulence and that these structures might be the primary mechanism for the generation of jet noise. A number of subsequent investigations have focused on this approach with the hope that this regular pattern, if any, and its role in jet noise production could be better defined. Later, Becker and Massors[2] carried out a study on the vortex evolution and instability of an axisymmetrical jet with a Reynolds number range of 10^4. Crow and Champagne[3] performed measurements at a Reynolds number around 10^5 and reported that a large-scale orderly structure was observed within the noise-producing region of the jet. Based on these observations, they proposed a theoretical flow model consisting of axisymmetric vortex trains, with a preferred Strouhal number of 0.3 emerging by calculation. This model of an axial array of vortices was also recommended by other researchers[4,5,6] as the basic structure of a flow pattern designed to imitate the relatively periodic and deterministic behavior of turbulent round jets.

It is the purpose of this numerical investigation to verify and analyze the connection between the vortex model and the pressure field of a jet. There have been numerous studies of vortex rings; however, most of these concentrate only on a single vortex. The classical vortex ring of small cross-section in a perfect fluid[7] was physically unsatisfactory until the viscous effects were taken into account. By considering an inner viscous core and applying the boundary-layer technique, Tung and Ting[8] removed the mathematical singularity which is the essential drawback of the inviscid model. The same solution was obtained through an independent approach based on considerations of the kinetic energy and momentum balance of the fluid[9]. The interaction of two inviscid vortex rings was studied by Sommerfeld[10]; the viscous case was examined analytically by Gunzburger[12] and experimentally by Fohl and Turner[11]. By utilizing the viscous solution to formulate the vortex model into a train of axisymmetric vortex rings with viscous cores, Liu et al.[13] developed a combined theoretical and experimental program and obtained good qualitative comparisons between the estimation and the measured fluctuations of the pressure field of a jet. The numerical simulation reported here is undertaken as a further test of the validity of the proposed vortex ring model. The fluctuation characteristics of the pressure signals are modeled by the random generation of a train of vortex rings. Statistical explanations to random behaviors of the pressure field of a jet will be the main emphasis of the present investigation.

FORMULATION

Let $[R(t), Z(t)]$ be the position of an isolated vortex ring at time t in an axisymmetric cylindrical coordinate system (r,z) with z coinciding the axis of symmetry of the ring, and r_1 and r_2 be the shortest and longest distance from the point of interest P to the center of the vortical core (see figure 1). Within the framework of the classical inviscid theory, the well-known stream function[7] for a potential flow induced by an axisymmetric planar vortex ring is

$$\psi = -\frac{\Gamma}{2\pi}(r_1 + r_2)[K(\frac{r_2 - r_1}{r_2 + r_1}) - E(\frac{r_2 - r_1}{r_2 + r_1})] \qquad (1)$$

Here K and E are the complete elliptical integrals of the first and second kind, and $\Gamma(t)$ the total circulation around the ring. The corresponding induced velocities at P in r- and z-direction are, respectively,

$$W_1 = \frac{1}{r}\frac{\partial\psi}{\partial z}$$

$$W_3 = -\frac{1}{r}\frac{\partial\psi}{\partial r} \qquad (2)$$

The well-known deficiencies of this inviscid formulation arise from the undefined vortical core and the singularity of the velocity at the center of the core.

Obtained by considering a viscous inner core in a region of large velocity gradients[8], the equation of motion for a vortex ring submerged in an irrotational inviscid flow stream is

$$\dot{Z} = \frac{\Gamma(t)}{4\pi R}\{\log \frac{8R}{\delta} - 0.558\} \tag{3}$$

Here the dot represents the derivative with respect to t. The symbol δ is the effective radius of the viscous core defined as:

$$\delta = 2\sqrt{\nu\tau} \tag{4}$$

and is assumed to be much smaller than the radius of curvature R. The quantity ν is the viscosity and τ is a time scale defined by the integral equation

$$\tau(t) = \int_{t_0}^{t} R(s)ds/R(t) \tag{5}$$

where t_0 is the creation time of the vortex ring.

The intention of this numerical study is to sumulate the fluctuations of the pressure field near a jet by means of a flow model consisting of a train of coaxial axisymmetric vortex rings with viscous cores submerged in an inviscid uniform stream. The stream velocity U_∞ is either taken as one-half of the jet velocity or regarded as a parameter in order to fit the experimental data.

The measured pressure signals to be simulated, shown in figure 2, were obtained from the experiment given in reference 13.

The experimental setup (figure 3) consists of a jet nozzle pointing upwards and a vertical array having twelve microphones located just outside the boundary of the jet[13]. In the present simulation, the region of interest is restricted to that of the experimental measurements where the convective speeds are small in comparison with the sound speed. The implication is the Laplace equation dominates over the acoustics wave equation, and is, therefore, adequate to describe the flow field by the incompressible potential solutions. (This assumption of incompressibility is reasonable in the present case since compressibility does not alter the turbulence structure until the mean velocity greatly exceeds the sonic speed[14]). It is further hypothesized that the overall contribution to the flow field by a train of vortex rings can be approximated by superposing the contribution of individual vortex rings, and hence no merging mechanisms will be considered.

Let the subscripts k and i denote the quantities associated with the k-th and i-th rings, respectively. As an extension of the investigation for the interaction of a pair of vortex rings[12], the governing equations of motion of the k-th ring in the presence of the i-th one are as follows:

$$\dot{R}_k(t) = \sum_{i=1}^{N} W_{1i}(t, R_k, Z_k)$$

$$\text{for } i \neq k \qquad (6)$$

$$\dot{Z}_k(t) = \sum_{i=1}^{N} W_{3i}(t, R_k, Z_k) + U_\infty + \frac{\Gamma_k}{4\pi R_k}\{\log \frac{8R_k}{\delta_k} - 0.558\}$$

where W_{1i} and W_{3i}, defined by equations (2), are the induced velocities by the presence of other vortex rings. The number of active vortices N is a parameter to be obtained by matching with the experimental data, and U_∞ is the uniform stream velocity which is taken as equal to half of the jet efflux velocity, U_j. Assume that the k-th ring starts rolling up at the shedding time t_k with a linear strength proportional to $U_\infty U_c$, U_c being the convection velocity of the ring. The circulation reaches a saturated value at the shedding time of the (k+1)-th vortex ring, t_{k+1}. It is also assumed that, beginning at a certain distance Z_{max} downstream of the jet, the circulation of the ring decays with a linear rate less than the rolling-up strength and that the ring vanishes when its circulation reaches zero. The basis of this hypothesis for the growth and decay of vortex rings will be given in the next section. The evolution of the circulation is described by the following equation (see figure 4).

$$\Gamma_k(t) \sim U_\infty U_c \; f_k(t) \tag{7}$$

Here $$f_k(t) = \begin{cases} 0 & 0 \le t < t_k \\ t - t_k & t_k \le t < t_{k+1} \\ t_{k+1} - t_k & t_{k+1} \le t < t_k^* \\ t_{k+1} - t_k - \alpha(t - t_k^*) & t_k^* \le t < t_k^{**} \\ 0 & t_k^{**} \le t < \infty \end{cases}$$

t_k^* = the time when the center of the k-th vortex ring reaches the distance Z_{max} downstream. Z_{max} is a parameter to be obtained by matching with the experimental data.

$t_k^{**} = \frac{1}{\alpha}(t_{k+1} - t_k) + t_k^*$, the time of complete destruction of the k-th vortex ring, i.e., $\Gamma_k(t_k^{**}) = 0$.

α = a parameter which governs the decay of the vortex ring, ranging over values between 0 to 1.

Equations (6) will be solved subject to the initial conditions

$$R_k(t_k) = D/2$$
$$Z_k(t_k) = 0 \qquad (8)$$

at the nozzle of the jet.

The simulation of the real-time pressure distribution measured near a jet is to be made along the cone of measurement in the experiment[13], which is outside of the diffusive cores of all the vortex rings at all times. The classical Bernoulli solution is then applicable since the region of interest is practically irrotational and inviscid. The induced velocity potential[7] for a train of coaxial axisymmetric vortex rings is

$$\phi = -\frac{1}{2}\sum_{i=1}^{N}\Gamma_i R_i\int_0^\infty e^{-\kappa|z-Z_i|}\,\mathrm{sgn}(z-Z_i)\,J_0(\kappa r)\,J_1(\kappa R_i)\,d\kappa \qquad (9)$$

where J_0 and J_1 are the Bessel function of the first kind of order 0 and 1 respectively. The corresponding pressure variation, obtained with the use of the boundary condition that the incompressible uniform stream remains unperturbed at a distance sufficiently far away from the vortex rings, is given by

$$-\frac{\Delta p}{\rho} = \frac{p_\infty - p}{\rho} = \frac{\partial \phi}{\partial t} + \frac{1}{2}\left[\left(U_\infty + \sum_{i=1}^{N} W_{3i}\right)^2 + \left(\sum_{i=1}^{N} W_{1i}\right)^2\right] - \frac{1}{2}U_\infty^2 \qquad (10)$$

where ρ is the density of the fluid (assumed to be constant) and p_∞ is the mean pressure outside the perturbed region. The summations in equations (9) and (10) are taken over all the active vortex rings within the region of interest.

The theoretical model under consideration is based on equations (6) and (10). The instantaneous positions of the vortex rings and the induced pressure fluctuations can be obtained by numerical integration of these equations, subject to the initial conditions (8).

BASIS FOR THE SIMULATION

The dominant parameters of the simulation based on the preceding mathematical formulation are U_∞, the uniform stream velocity; ν, viscosity; $\Gamma(t)$, circulation of the vortex rings; and t_k, the shedding time of the vortex rings. These parameters are chosen with reference to the experimental observations.

Viscosity

Viscosity enters the simulation in terms of the viscous core defined by equation (4). There is not much detailed evidence on the growth of vortical cores for the ring type structure of jets except that reported by Lau and Fisher[6], who estimated the vortex core radius to be one-tenth or less of the jet diameter at an axial position two diameters downstream of the jet exit. The viscosity, equal or less than 0.01 m^2/sec for the present simulation, is therefore chosen such that the vortical core possesses the above-estimated growth rate.

Circulation

The time-history of circulation of vortex rings described by equation (7) is constructed based on the shear strength in the mixing layer close to the jet exit and the experimental observations of the vortex ring type structure downstream of turbulent jets. For simplicity let the convective rate of increase of the circulation equal to the average shear strength at the jet exit, i.e., U_∞, and let this rate of increase remain constant as the vortex ring travels downstream with a convection velocity U_c. The circulation reaches a saturated value at the shedding time of the successive vortex ring, t_{k+1}. The creation of the circulation described by equation (7) is then followed.

The assumption on the decay of the circulation of vortex rings starting at a certain distance downstream of the jet is based on the fact that vortex ring type structures and their corresponding pressure signals are seldom observed beyond the potential core. According to the experimental observation[2,3], vortex type patterns start dissipating no further than four diameters downstream from the jet exit. The distance of Z_{max} in this simulation is therefore chosen to be three diameters or less. The vorticity then dissipates, under the viscous influence, with a linear rate governed by the parameter α to be obtained by matching with the experimental data.

Random Shedding Time

The large-scale vortex puffs were generated randomly in time[3]; an observation which is consistent with the random nature of the measured pressure field. The present simulation of the random shedding time between successive vortex rings are estimated based on the time intervals between successive peaks of pressure of fluctuations as measured in the experiment[13]. The simulated pressure is then compared with the measured pressure fluctuations from which this numerical input is obtained. Second, a numerical program is used to generate random vortex shedding time intervals having probability distribution similar to that of the intervals between successive pressure peaks measured in reference 13. This requirement for similar probability distribution provides a statistical similarity of peak variations and characteristics between the time-history measured pressure and its corresponding simulation.

RESULTS AND CONCLUDING REMARKS

Numerical results for the time-history of the pressure in the vicinity of a jet, with the time intervals between peaks at one diameter downstream used as input to the numerical model, are plotted in figures 5 along with the experimental pressures. No attempts were made on matching their amplitudes because of the random nature of the pressure fluctuations. Direct comparisons on pressure peaks are impossible even for two pieces of record obtained from the same set of experiment. Statistical analysis appears to be the most sensible comparison.

Figure 6 shows the simulated pressure fluctuations calculated by inputing three hundred random shedding time intervals having probability distribution similar to that of the intervals between experimental pressure peaks at the one diameter downstream station. Statistical comparisons between these numerical results and the experimental measurements[13] are made at several stations along the cone of measurement. Figures 7 display comparisons of the probability distributions of the time intervals between calculated and experimental pressure peaks for several values of Z/D. Good qualitative agreement on the envelops of the probability distribution and the most probable time intervals (interval with maximum number of counts) between pressure peaks is observed. The experimental samples outnumber the numerical ones by the ratios indicated in figures 7. Improvements on the numerical part will be expected if more numerical samples are considered.

The variation of the most probable time intervals between pressure peak obtained from the distribution curves in figures 7 is plotted versus the downstream stations along the cone of measurement. The numerical results show good agreement with their experimental counterparts. No comparison beyond the potential core was made since vortex ring type structures are rarely seen there. As shown by the experimental data, the slope of the most probable time intervals beyond the potential core is different from that within the potential core. These two slopes intersect at a distance 4D downstream with a corresponding Strouhal number equal to 0.3, an important location and number for the emission of sound[3]. This suggests a possible geometry changed for the axisymmetric structures. Nonasisymmetric and nonplanar components are believed to play an important role beyond the potential core, and are now being incorporated into the model in order to allow simulation further downstream of the jet exit.

REFERENCES

1. Mollo-Christensen, E. (1967), J. of Applied Mech., Trans. of ASME.

2. Becker, H. A. & Massaro, T. A. (1968), JFM, Vol. 31.

3. Crow, S. C. & Champagne, F. H. (1971), JFM, Vol. 48.

4. Lau, J. C., Fisher, M. J. & Fuchs, H. V. (1972), J. of Sound and Vibration, Vol. 22.

5. Laufer, J., Kaplan, R. E. & Chu, W. T. (1973), AGARD-CP-131.

6. Lau, J. C. & Fisher, M. J. (1975), JFM, Vol. 67.

7. Lamb (1932), Hydrodynamics, Dover Publications, Inc., N. Y.

8. Tung, C. & Ting, L. (1967), Phys. of Fluids, Vol. 10.

9. Saffman, P. G. (1970), Studies in Appl. Math., Vol. XLIX, No. 4.

10. Sommerfeld, A. (1950), Mechanics of Deformable bodies, Academic Press, N. Y.

11. Fohl, T. & Turner, J. S. (1975), Phys. of Fluids, Vol. 18.

12. Gunzburger, M. D. (1972), J. of Eng. Math., Vol. 6.

13. Liu, C. H., Maestrello, L. & Gunzburger, M. D. (1976), Progress in Astronautics & Aeronautics, Vol. 43, AIAA & MIT Press.

14. Ffowcs-Williams, J. E. (1963), Phil. Trans. Roy. Soc. A 255.

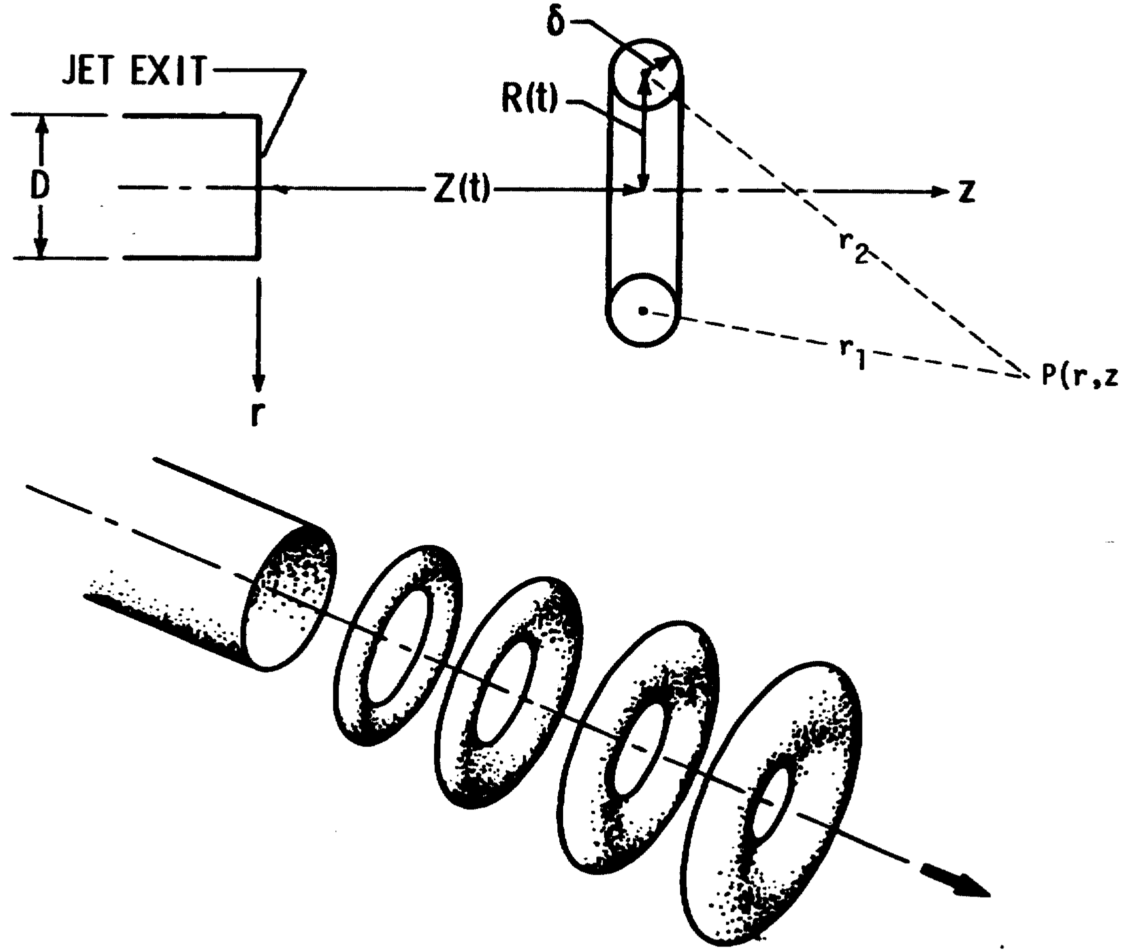

Figure 1. Geometry of vortex rings.

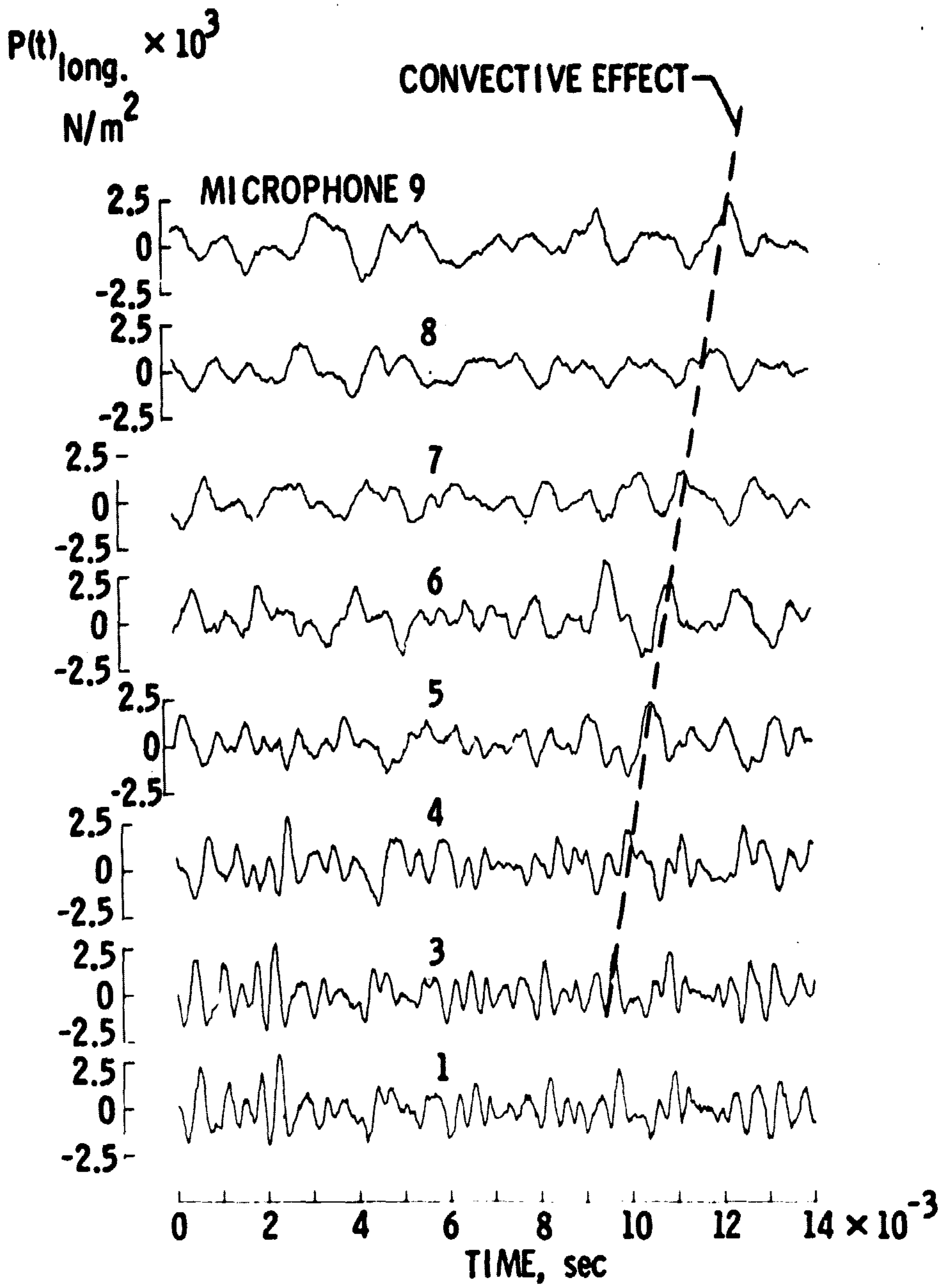

Figure 2. Time-history of the measured pressure signals at several stations.

VERTICAL ARRAY

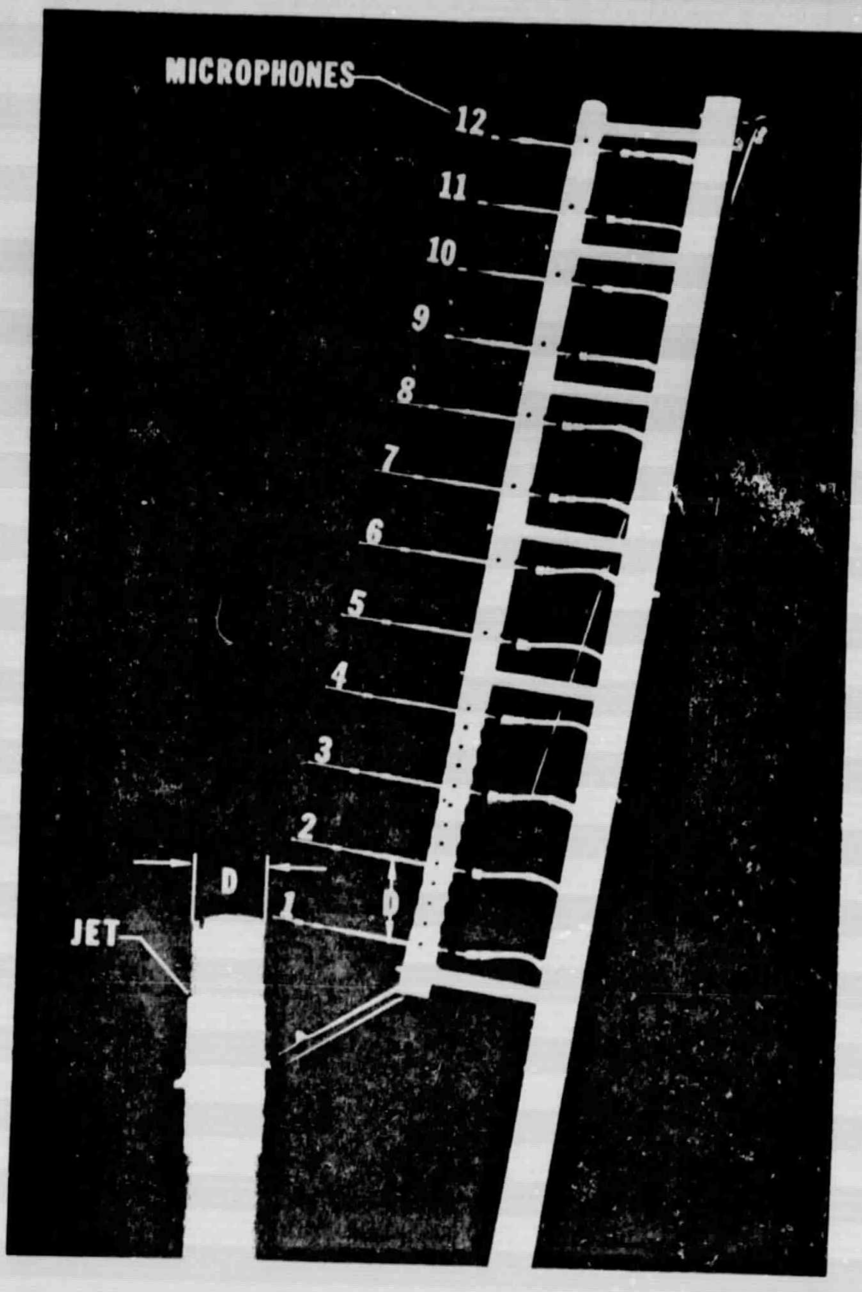

Figure 3. Experimental setup.

t_k = Time at which the k^{th} vortex ring is shed

t_k^* = Time at which $Z_k(t) = Z_{max}$

t_k^{**} = Time at which $\Gamma_k(t) = 0$

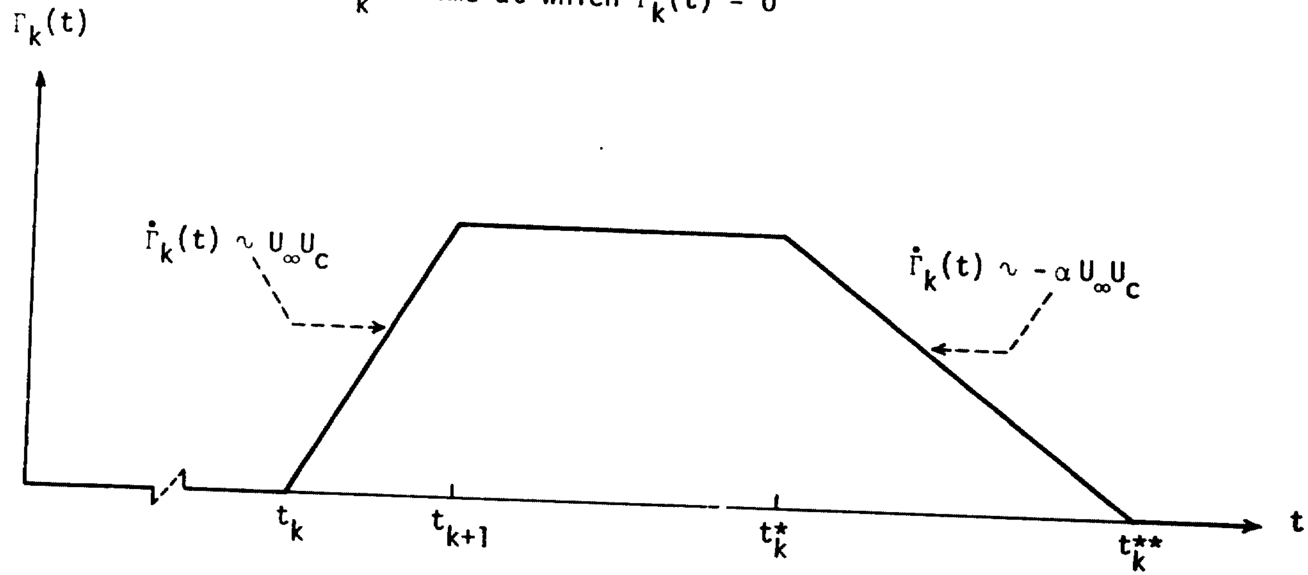

Figure 4. Time-history of the circulation of the k^{th} vortex ring.

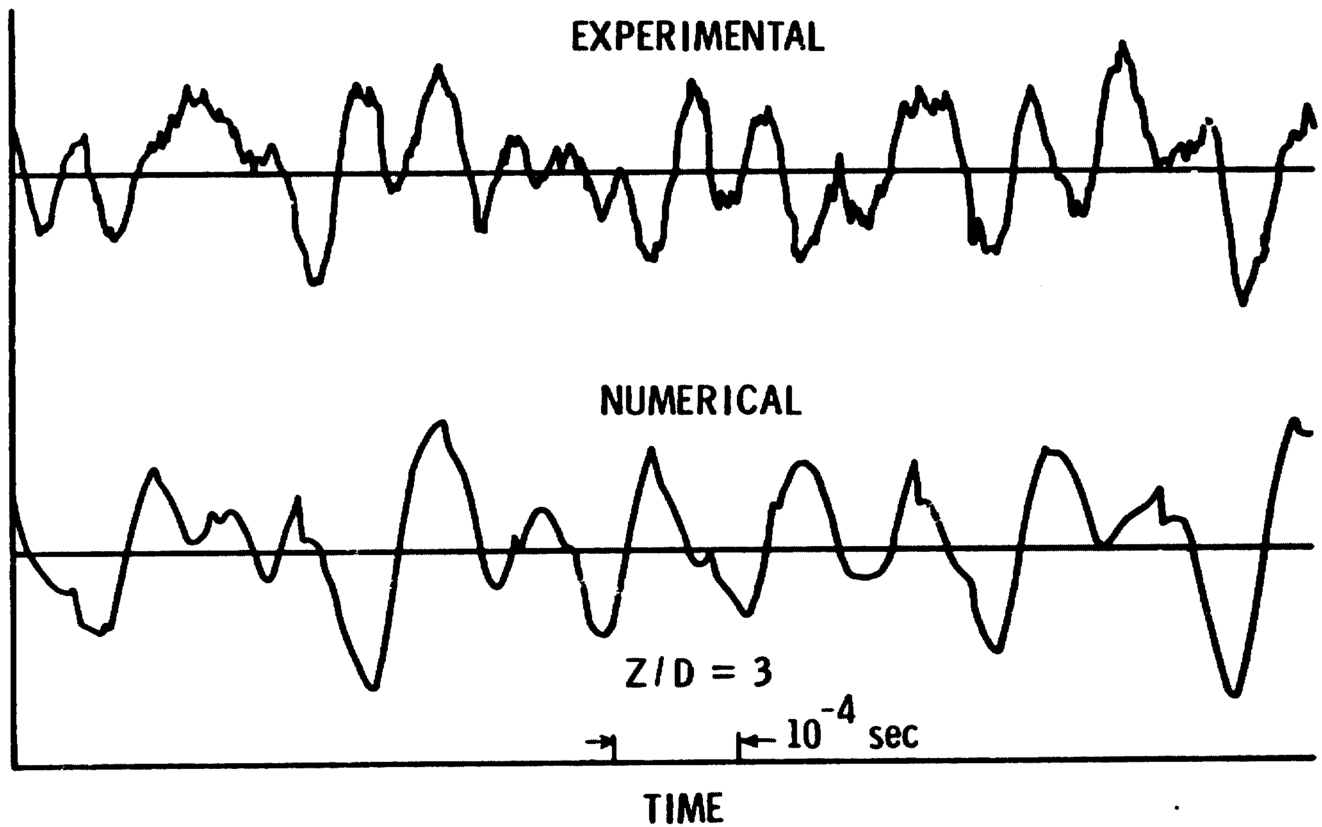

Figure 5a. Pressure comparison between the simulation and the time-history measurements at 3D downstream.

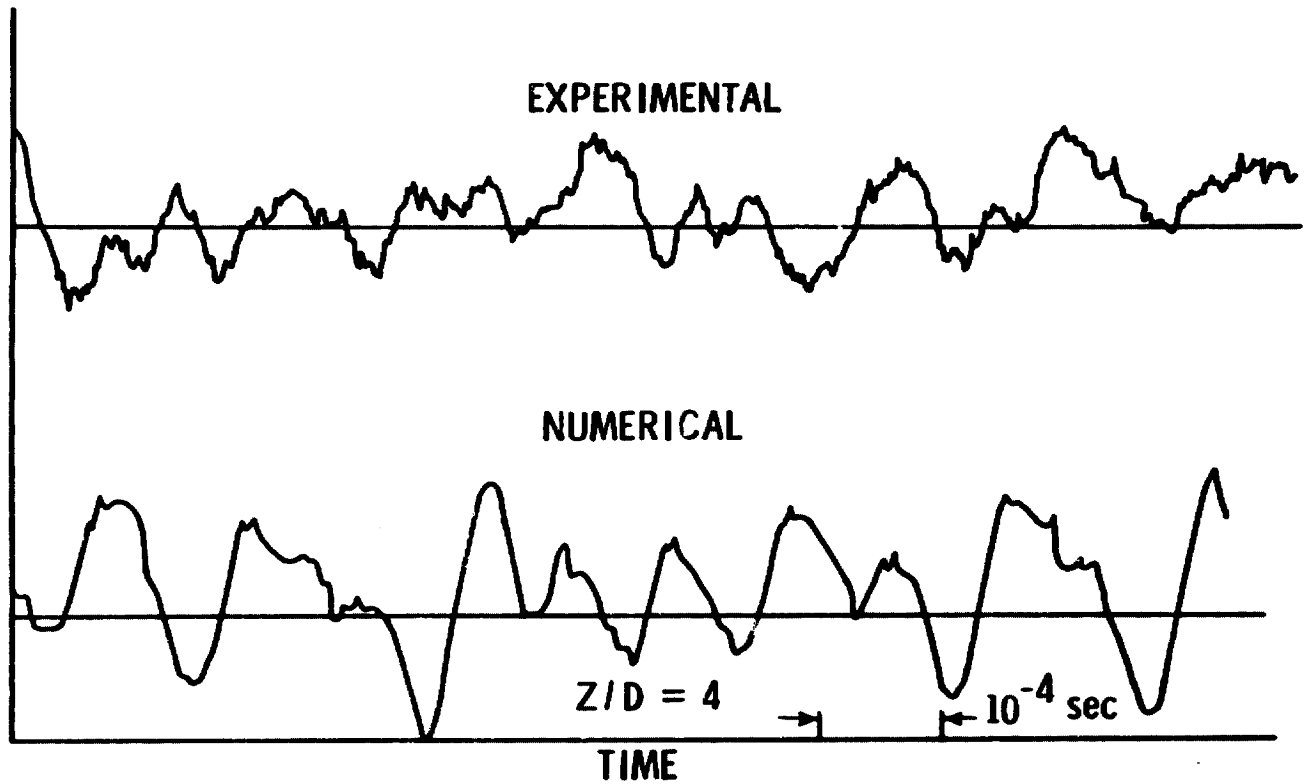

Figure 5b. Pressure comparison between the simulation and the time-history measurements at 4D downstream.

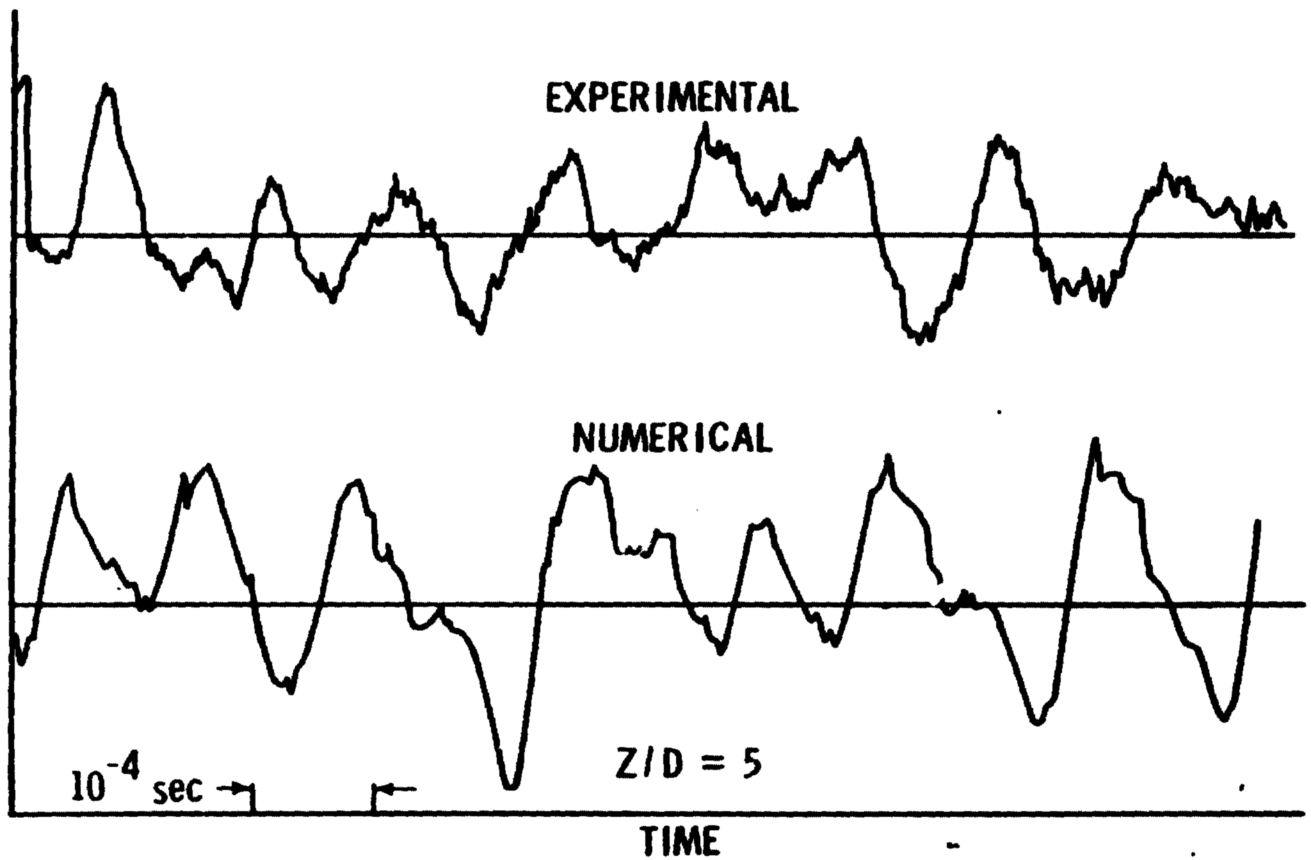

Figure 5c. Pressure comparison between the simulation and the time-history measurements at 5D downstream.

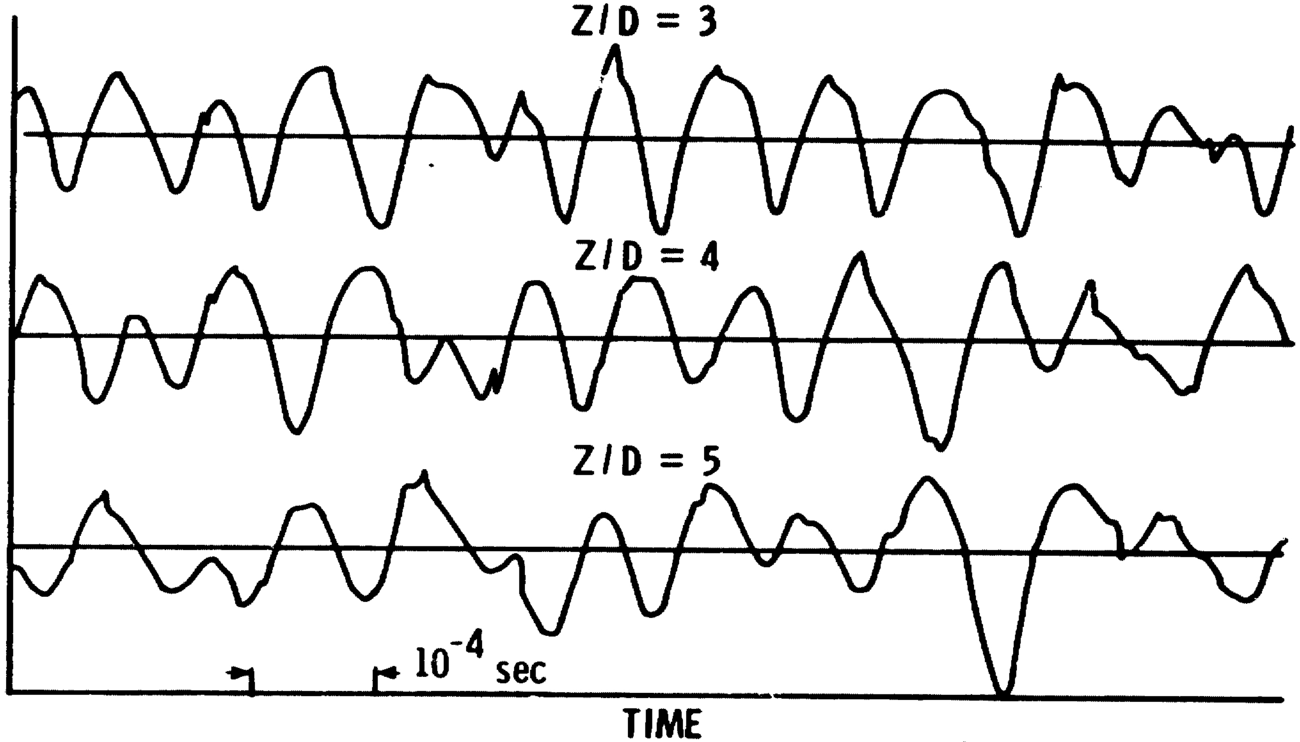

Figure 6. Simulated pressure fluctuations by randomly shed vortex rings at downstream stations, (U_∞ = 110 m/sec).

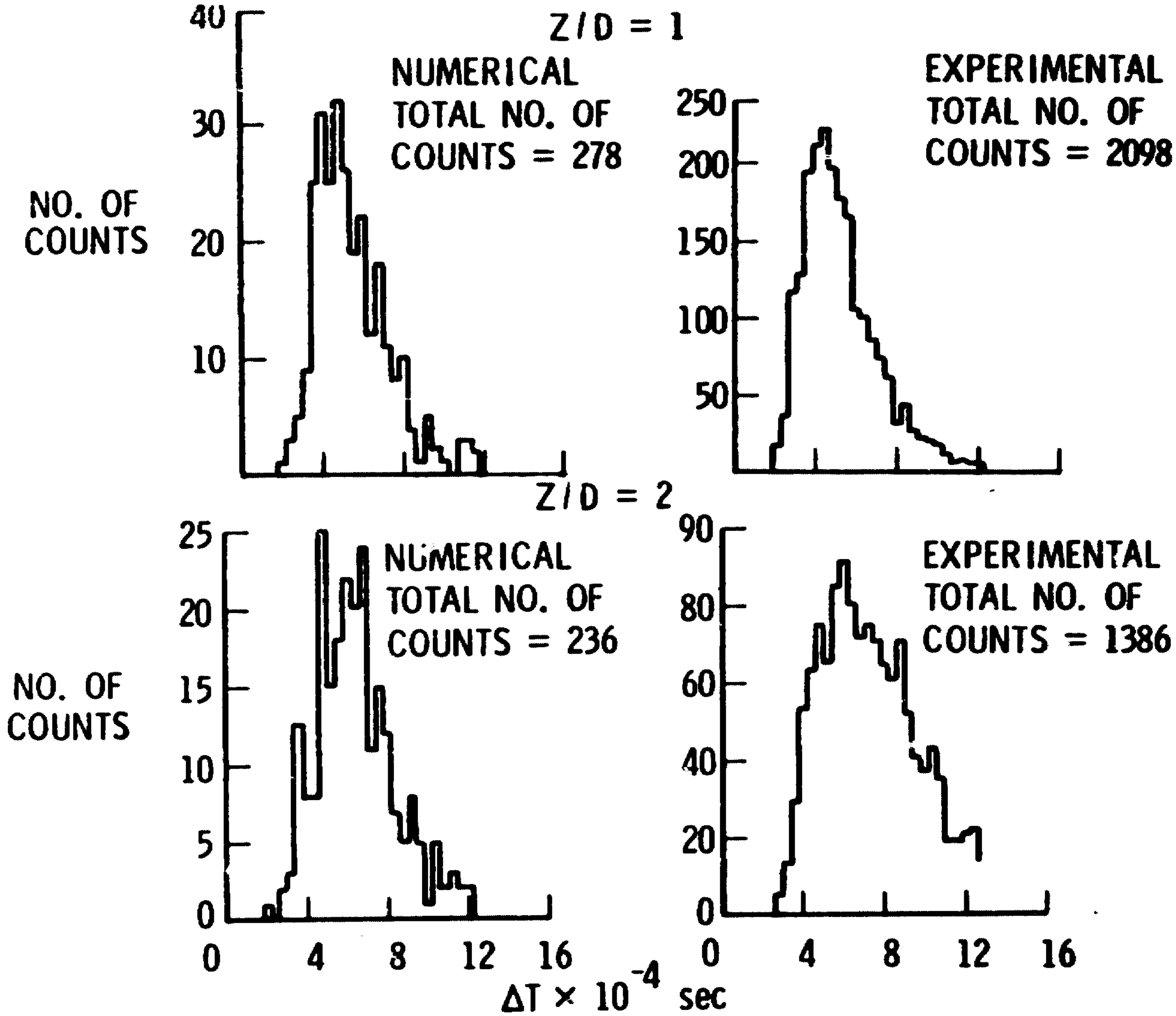

Figure 7a. Statistical comparisons of the probability distribution of the time interval between successive pressure peaks.

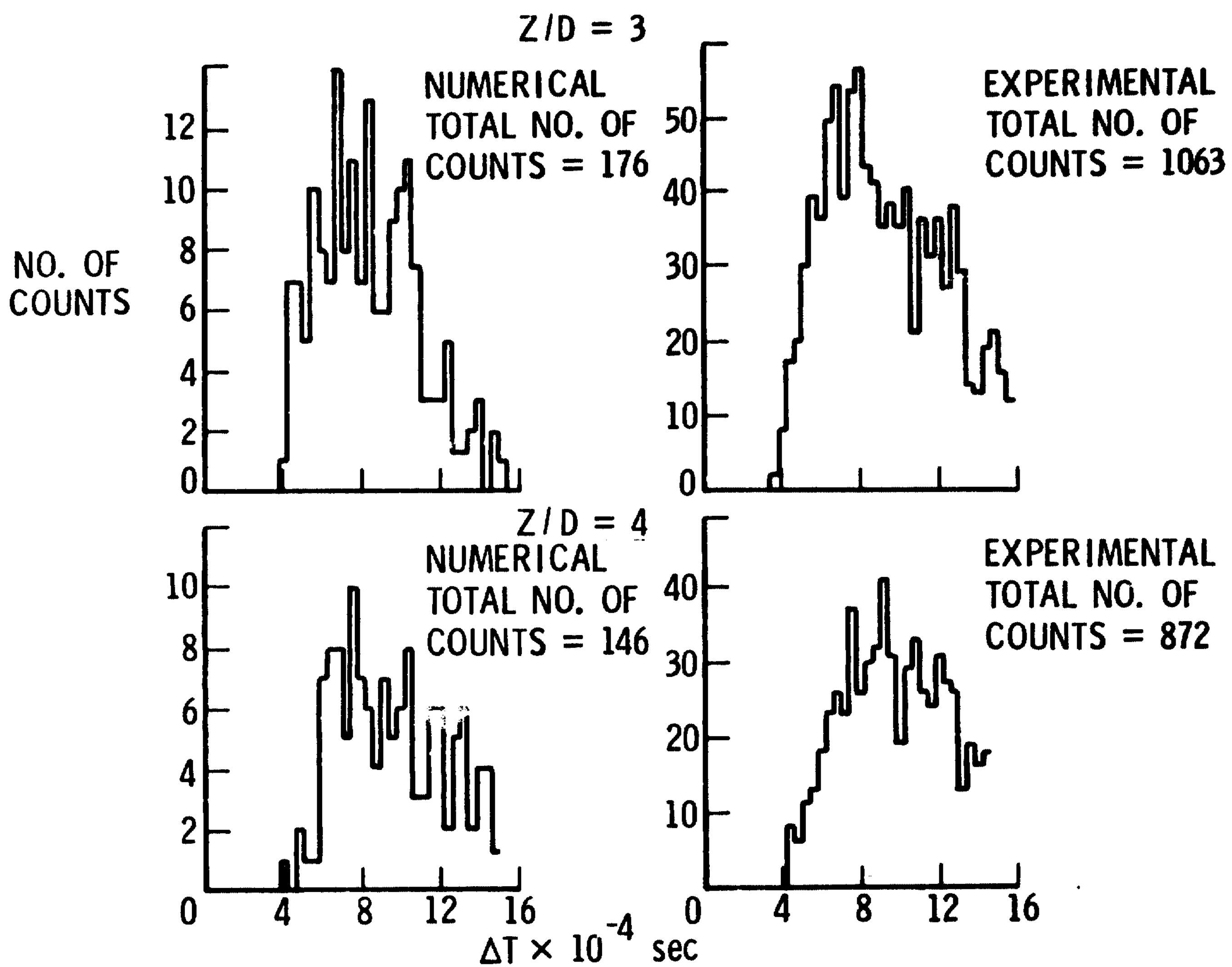

Figure 7b. Statistical comparisons of the probability distribution of the time interval between successive pressure peaks.

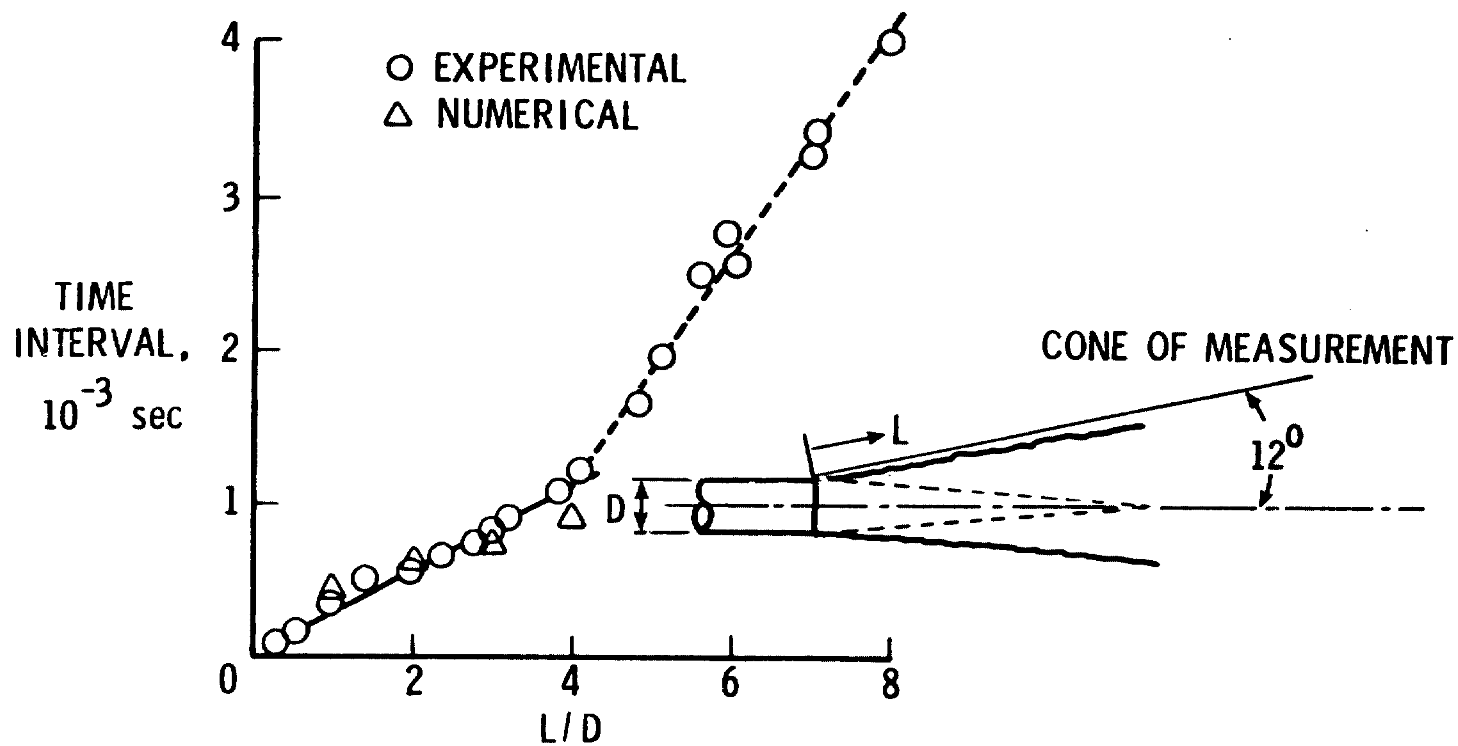

Figure 8. Variations of the most probable peak time interval along the cone of measurements.